Hindawi
Journal of Nanotechnology
Volume 2022, Article ID 5474645, 6 pages
https://doi.org/10.1155/2022/5474645

Research Article

Green Synthesis of Iron Oxide Nanoparticles Using *Hibiscus rosa sinensis* Flowers and Their Antibacterial Activity

F. Buarki,[1] **H. AbuHassan**,[1] **F. Al Hannan**,[2] **and F. Z. Henari**[2]

[1]*Royal College of Surgeons in Ireland, Medical University of Bahrain, Busaiteen, Bahrain*
[2]*Department of Medical Sciences, Royal College of Surgeons in Ireland, Medical University of Bahrain, Building 2441, Road 2835, Block 228, Busaiteen, Bahrain*

Correspondence should be addressed to F. Z. Henari; fzhenari@rcsi.com

Received 22 November 2021; Revised 2 February 2022; Accepted 16 February 2022; Published 10 March 2022

Academic Editor: Brajesh Kumar

Iron oxide nanoparticles (α- Fe_2O_3) were synthesized using an unconventional, eco-friendly technique utilizing a *Hibiscus rosa sinensis* flower (common name, China rose) extract as a reducer and stabilizer agent. The microwave method was successfully used for the synthesis of iron oxide nanoparticles. Various volume ratios of iron chloride tetrahydrate to the extract were taken and heated by the microwave oven for different periods to optimize iron oxide nanoparticle production. The synthesized iron oxide nanoparticles were characterized using the ultraviolet-visible spectrometer (UV-Vis), Fourier transform infrared spectroscopy (FTIR), transmission electron microscopy (TEM), and X-ray diffraction (XRD). X-ray diffraction confirmed the formation of α-Fe_2O_3 nanoparticles (hematite). The average size of iron oxide nanoparticles was found to be 51 nm. The antibacterial activity of the synthesized iron nanoparticles was investigated against different bacteria such as *Staphylococcus aureus*, *Pseudomonas aeruginosa*, *Klebsiella pneumonia*, and *Escherichia coli*. The results showed that the synthesized iron nanoparticles exhibited an inhabitation effect on all studied bacteria.

1. Introduction

Metal nanoparticles gain great attention due to their wide range of applications in the fields of electronics, optoelectronics, antibacterial activity, and medical applications such as therapy, diagnosis, and drug delivery [1–3]. The development of adequate techniques for synthesizing metal nanoparticles has become a major focus of researchers. Diverse methods have been developed and utilized for synthesizing metal nanoparticles, such as chemical, physical, and green methods. The chemical method involves chemical agents, resulting in a large amount of chemical waste as a byproduct, resulting in environmental contamination issues. Physical methods such as gamma irradiation, pulse laser ablation, and spark discharge are used to synthesize nanoparticles, and these methods are effective; however, they require relatively expensive apparatus. Green methods involving plant extracts, bacterial, and fungal forms are the most considered to produce various metal nanoparticles [4, 5]. These methods are environmentally safe, with short production times and low costs compared to other methods. The synthesis of metal nanoparticles from plant extracts is considered an easy process relative to fungal/bacteria cultures since fungal and bacterial cultures require sterilized conditions and skills to preserve. Furthermore, the plant extracts used to synthesize the nanoparticles show various size and shape distributions.

Green synthesis involves using plant extracts from *Hibiscus cannabinus* leaves [6] and cinnamon bark [7, 8]. Plant extracts usually contain sugars, terpenoids, polyphenols, alkaloids, phenolic acids, and protein, which are responsible for reducing and stabilizing metal nanoparticles [9]. It has been confirmed that the functional groups, such as –C–O–C–, –C–O–, –C=C–, and –C=O–, present in the phenolic compounds can assist in the formation of metallic nanoparticles [10]. Various types of iron/iron oxide (Fe/FeO-NPs) have been synthesized using extracts from plants and their parts, such as roots, leaves, fruits, flowers, bark,

stems, and seeds. [11–13], and they have been investigated for their use in photocatalysis and the elimination of various organic dyes in wastewater [14]. However, a few studies are available with the hematite iron oxide phase compared to other iron oxide phases. The reported studies are on photocatalytic degradations and domestic wastewater treatment. None of these studies revealed the antibacterial activity of α-Fe_2O_3 nanoparticles [12].

In this study, we report the synthesise of iron oxide nanoparticles (α- Fe_2O_3 NPs) using iron chloride tetrahydrate as a precursor. The various phytochemicals present in the *Hibiscus rosa sinensis* flower leaves act as reducing and capping agents for the synthesis of NPs [10]. After mixing flower leaf extract with iron chloride tetrahydrate at certain reaction conditions. The phytochemicals that exist in the extract cannot reduce Fe2+ to Fe0; instead, they react with the iron ions to give iron oxide NPs, as Fe is susceptible to oxidation. The brown colour formation occurred due to the interaction between these phytochemicals and metal ions, ensuring the formation of α-Fe_2O_3 nanoparticles [15]. Iron oxide nanoparticles of hematite (Fe_2O_3 NP) were selected for their stability, anticorrosive properties, and tunable magnetic and optical properties over other iron oxide phases. They can be synthesized by the green method in various shapes and with a broad size range [16]. The microwave heating and the adjustment of the volume ratio of the precursor to the plant extract were investigated to optimize the production of iron oxide nanoparticles. The existence of nanoparticles was confirmed by using UV-Vis spectrometry, TEM, FTIR, and X-ray diffraction. The nanoparticle stability was studied over two weeks by monitoring the surface plasmon resonance peak using a UV-Vis spectrometer. The synthesized iron oxide nanoparticles were used to investigate antibacterial activities on different mycobacterial species such as *Staphylococcus aureus*, *Pseudomonas aeruginosa*, *Klebsiella pneumonia*, and *Escherichia coli*.

2. Materials and Methods

2.1. Synthesis of Fe_2O3 Nanoparticles. *Hibiscus rosa sinensis* flowers were collected from a local garden, washed several times, and rinsed with distilled water to remove dust particles. The washed flowers were dried in an oven at a temperature of 60°C for 24 hours. The dried flowers have been ground down, and 5 g of ground hibiscus dissolved in 100 ml of double-distilled water. The mixture boiled for five minutes. After settling for an hour, the extract was filtered twice using Whatman No.1 filter paper. The chemical used was iron chloride tetrahydrate ($FeCl_24H_2O$) of high purity and analytical grade, purchased from Sigma-Aldrich (Sigma-Aldrich 220299).

0.02 g of iron chloride tetrahydrate was dissolved in 100 ml of distilled water to prepare 1 mM of $FeCl_24H_2O$ solution. The synthesis of iron nanoparticles was achieved by mixing 1 mM FeCl24H2O and *Hibiscus rosa sinensis* flower extract in three different volume ratios: 5 ml of $FeCl_24H_2O$ and 5 ml of extract (1 : 1), 5 ml of $FeCl_24H_2O$ and 10 ml of extract (1 : 2), and 5 ml of $FeCl_24H_2O$ and 15 ml of extract (1 : 3). The mixtures were placed in different clean sterilized Erlenmeyer flasks. The mixtures of varying volume ratios were subjected to heat by microwave for different time durations. The best result was obtained when the mixture was exposed to heat for 20 seconds. Other volume ratios of larger extract volumes than the iron salt were used for synthesizing iron oxide nanoparticles. It was found that the ratio of 1 volume of $FeCl_24H_2O$ to 2 volumes of the extract gives better results in the relation of surface plasmon resonance (SPR) peak and stability of the nanoparticles. The experiments were accomplished at pH 7, and no pH control was applied. The synthesized nanoparticles stability was evaluated using UV-Vis absorption spectra and found to be stable for over two weeks. Solution of 1 : 2 volume ratios was centrifuged at 3000 rpm for 30 minutes, the supernatant discarded, and the pellet washed with distilled water and centrifuged again. This process was repeated three times to remove any impurities. The synthesized Fe_2O_3NPs powder was subjected to various characterizations.

2.2. Sample Characterization. The synthesized Fe_2O_3 NPs were exposed to various characterization methods to identify their specific properties. For optical properties, Shimadzu's UV-1800 UV-Vis spectrometer was used to record the absorption spectrum to identify the surface plasmon resonance (SPR) band. TEM was used to determine the size and shape of Fe_2O_3 NPs. The functional groups were identified by recording the FTIR spectrum using an Alpha BRUKER Transmission Spectrometer from Pike Technologies. The structural, elemental composition, and particle size of the Fe_2O_3 NPs were characterized by using XRD. Other characterization methods such as XPS, FESEM, EDX, HRTEM, and VSM were not carried out because of unavailability to the authors.

2.3. Antibacterial Activity. Fe_2O_3 NPs tested for their antibiotic sensitivity pattern against different types of Gram-positive and negative pathogens, which are known to develop antibiotic resistance, such as *Escherichia coli*, *Klebsiella pneumonia*, *Staphylococcus aureus*, and *Pseudomonas aeruginosa*. Colonies from different types of bacteria were inoculated in L.B. broth and incubated for 24 hours at 37°C in an incubator. The bacterial cultures were then diluted to 1 : 100 (equivalent to a cfu of 10^8). A 50–100 μL of the bacteria was taken, and a streak was made on nutrient agar (L. B. agar) medium using a sterile spreader in all directions. The antibiotic disks were applied with aseptic precautions. The disks were soaked in different samples of iron oxide nanoparticles and extracted and placed with centers at least 30 mm apart. The plate was incubated at 37°C in an incubator for 24 hrs. After incubation, the zone of inhibition around the disks was observed and measured.

3. Results and Discussion

3.1. UV-Vis Spectroscopy. The synthesis of iron oxide nanoparticles using *Hibiscus rosa sinensis* flower extract was preliminarily confirmed by a characteristic change of the colour of the extract solution from yellow to a dark brown

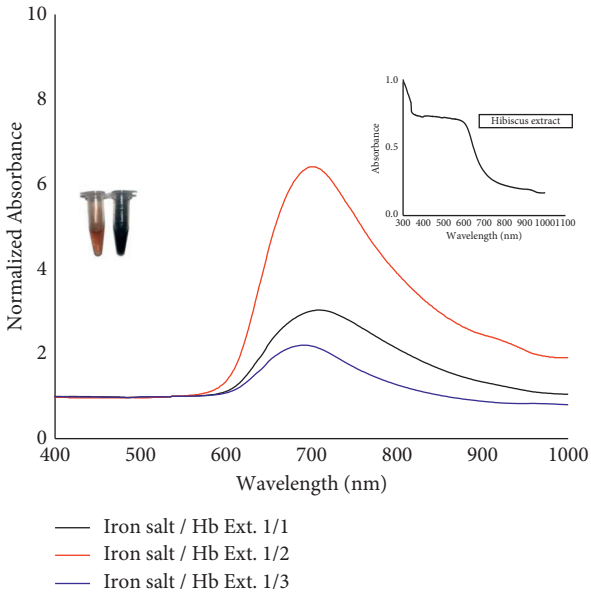

Figure 1: UV-Visible spectra of Fe_2O_3 nanoparticles, *Hibiscus rosa sinensis* flowers, and colour of extract solution from yellow to dark brown.

solution when the iron salt solution was added [15] (Figure 1). The absorbance spectra of the solution were recorded at a 200–1000 nm wavelength range. The formation of an SPR band was observed. The position of the SPR band depends on the particle size and shape, the aggregation state of the nanoparticles, and the dielectric of the surrounding medium. Figure 1 shows the UV-Vis absorption spectra of the synthesized iron oxide NPS in various volume ratios of iron chloride tetrahydrate to hibiscus flower extract. The spectra demonstrated a characteristic peak surface plasmon resonance (SPR) band around 700 nm for all volume ratios, agreeing with the reported SPR for Fe_3O_4 NPs using hibiscus leaves [16]. The SPR arose from the collective oscillation of free electrons in the conduction band of iron oxide NPs. As shown in Figure 1, the highest absorption peak was observed for the volume ratio of 1 : 2. The observed high SPR may be due to larger particle sizes compared to other ratios. Haiss et al. [17] reported enhancement of the SPR peak for larger nanoparticles. No significant shift of the SPR peak was observed for different ratios of $FeCl_24H_2O$ to hibiscus extract. The UV-visible spectrum of the pure extract of hibiscus was recorded for comparison in Fig. [1]. As can be seen from Figure 1, the absorption peaks for hibiscus extracts are around 590 nm and 300 nm, which correspond to the existence of several natural compounds in the extract. These peaks vanished after reacting with an iron salt, indicating that the extract compounds acted as reducing and capping agents to synthesize the Fe_2O_3 nanoparticles. The sample absorption spectra were subjected to microwave heating for 20 seconds compared to those left at room temperature for 24 hours. Both samples' absorption were found to have almost similar characterization, with no significant difference in SPR peak location.

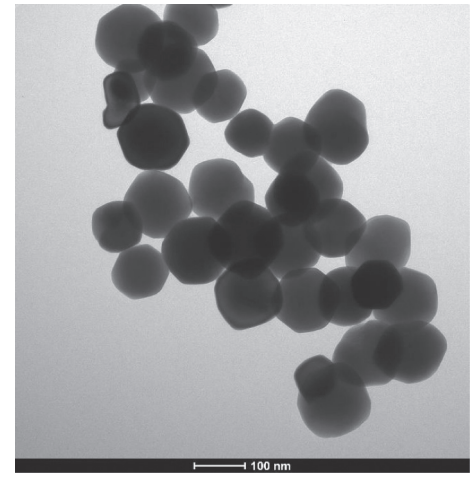

Figure 2: TEM image of Fe_2O_3 nanoparticles.

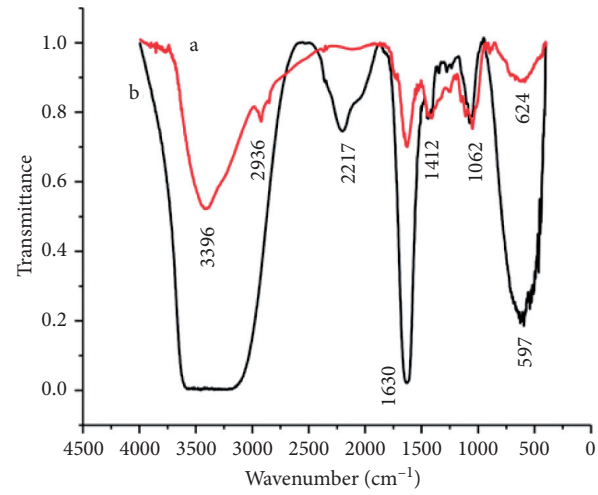

(a) Hibiscus extract
(b) Synth FeNPs

Figure 3: The FTIR measurements of (a) hibiscus extract and (b) caped Fe_2O_3 nanoparticles.

3.2. Transmission Electron Microscopy. Transmission electron microscopy (TEM) was performed to determine the shapes and sizes of iron oxide nanoparticles synthesized using *Hibiscus rosa sinensis* flower extract. The sample was prepared for TEM imaging by disbanding drops of the iron nanoparticle solution on a copper grid and left to dry at room temperature.

Figure 2 shows the TEM image of iron nanoparticles which reveals a polydispersity in shapes and sizes, with most nanoparticles of nearly spherical shape. The size distribution of nanoparticles was analyzed using ImageJ 1.5j software. The software converts pixels on the TEM images into nanometers by applying the scale of the image. From size analysis, the average size for Fe_2O_3 NPs was found to be in the range of 51 nm for a sample solution of 1 : 2 volume ratios.

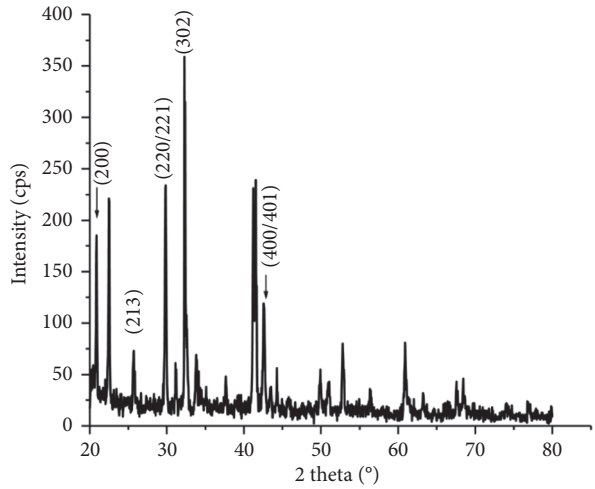

Figure 4: X-ray diffraction spectrum of Fe_2O_3 nanoparticle.

3.3. FTIR Measurements. The FTIR measurements were performed on the hibiscus extract and the synthesized Fe_2O_3 nanoparticle to identify a possible change in functional group bonds during the reduction process. As shown in Figure 3(a), the FTIR spectrum for hibiscus extracts displayed several strong bands around 624, 1062, 1412, 1630, 2215, 2936, and 3396 cm^{-1}. The same pattern was roughly observed for the synthesized iron oxide nanoparticles Figure 3(b). The shifted absorption band observed at 597 cm^{-1}, for the hibiscus extract band at 624 cm^{-1} corresponds to F–O stretches of Fe_2O_3, confirming the formation of nanoparticles. The observed absorption bands were higher in intensity than the extract, confirming the reducing role of the extract in the formation of Fe NPs. In Figure 3(a), the peak of 1062 cm^{-1} corresponded to the stretching vibration of C–O–C, polyphenol compounds present in the plant extract. 1412 cm^{-1} band quoted to the in-plane bending vibrations of OH in phenols. The absorption band at 1630 cm^{-1} related to the C=O bond stretching denotes the polyphenol compounds present in the plant extract and amino acids which stabilized and acted as a capping agent. Polyphenol compounds and phenyl groups play an essential role in reducing iron ions and then to iron oxide nanoparticles [15]. The band with higher intensity (Figure 3(b)) assigned to the OH groups indicates water-soluble polyphenols compound that have capped the surface of the prepared Fe NPs. The band at 2217 cm^{-1} may be due to C≡N stretching from unreacted impurities or due to CO_2 in the sample compartment. The band at 3353 and 2963 cm^{-1} corresponds to the OH bond stretching and denotes the aqueous phase, with an increase in the absorption band, indicating the ferric chloride reduction. It is worth mentioning that the same procedures were followed in preparing the extract and synthesized Fe_2O_3 NP samples concerning the weight used and the sample thickness. The existing findings agree well with the reported values in [17, 18].

3.4. XRD Study. Figure 4 shows the X-ray diffraction spectrum of the synthesized Fe_2O_3 NPs using the hibiscus extract. The spectrum was recorded at a speed scan of 1 degree per minute in a 2theta/theta range of 20–80 degrees at an X-ray wavelength of 1.54 nm. The indexed diffraction peaks shown in the figure represent the crystalline phase of Fe_2O_3NPs. The match of the peaks with D. B. card number 00-013-0458 for Fe_2O_3NPs confirms the synthesis of hematite α-Fe_2O_3 nanocrystals. The average crystallite size D was calculated by the Debye Scherrer equation $D = 0.9\lambda/\beta \cos \theta$), where λ is the wavelength of X-ray, θ is the Braggs angle in radians, and β is the full width at half maximum of the peak. The crystallite size D was found to be an average size of 36.4 nm. The results of the XRD analysis supported the tetragonal structure of α-Fe_2O_3 nanoparticles. By comparing the TEM and XRD size values, one concludes that there are multiple crystals in one particle in the case of single-crystal nanoparticles; the crystallite size and particle size are the same [19].

3.5. Antibacterial Activity of Iron Nanoparticles. The agar well diffusion method was used to evaluate the antimicrobial activity of phytogenic of Fe_2O_3 NPs against different bacteria strains such as *Staphylococcus aureus, Pseudomonas aeruginosa, Klebsiella pneumonia*, and *Escherichia coli.* As shown from Figure 5, the bacteria strains showed a zone of inhibition ranging from 2 to 6 mm. In Figure 5(a), the disc is divided into four different regions. Region one corresponds to iron oxide nanoparticles synthesized from a volume ratio of 1 : 2, while region 2 corresponds to iron oxide synthesized from a volume ratio of 1 : 1. Both synthesized iron oxide nanoparticles showed a maximum (3 mm) bacterial growth inhibition against *Staphylococcus aureus.* Regions 3 and 4 represent the control with zero inhabitation growth. Figure 5(b) shows a maximum (4 mm) bacterial growth inhibition against *Pseudomonas aeruginosa* for iron oxide nanoparticles synthesized from a volume ratio of 1 : 1 while for volume ratio 1 : 2 the maximum bacterial growth inhibition was 2 mm. Figure 5(c) shows 6 mm and 3 mm inhabitation zones against *Klebsiella pneumonia* for volume-ratios 1 : 1 and 1 : 2, respectively. Figure 5(d) shows 5 mm and 2 mm inhabitation zones against *Escherichia coli* for volume ratios 1 : 1 and 1 : 2, respectively. The observed tendency of antibacterial activity for different volume ratios may be related to nanoparticle size and the number of nanoparticles present in the solution. Haiss et al. [17] reported the enhancement of the SPR peak for larger nanoparticles. As can be seen from Figure 1, the SPR peak absorption for 1 : 1 is smaller than 1 : 2. Therefore, concluding that the nanoparticle size for 1 : 1 is smaller, smaller NPs have a larger surface area. This explains the more significant growth of inhabitation zones for *Pseudomonas aeruginosa, Klebsiella pneumonia,* and *Escherichia coli.* The nanomaterial activity increases with an increase in surface-to-volume ratio due to the decrease in nanoparticles' size [20]. However, the complete characterization of nanoparticles using TEM and DLS is needed to prove size-dependent antibacterial activities. The bacteria inhibition mechanism is still under investigation; some theories state that the nanoparticles invade the cell remembrance to

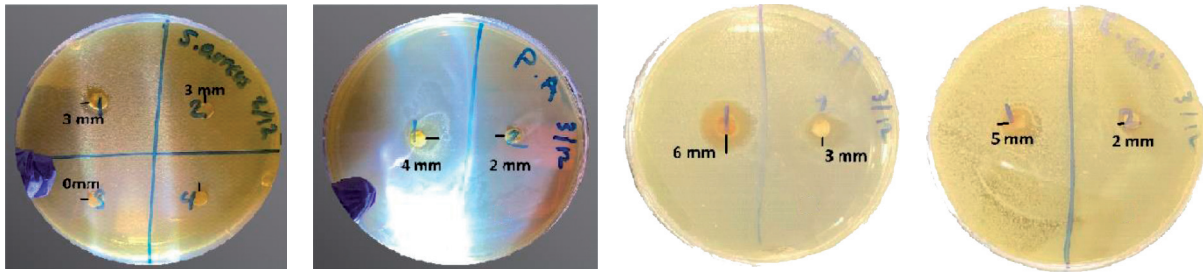

(a) (b) (c) (d)

Figure 5: Zone of inhibition of Fe_2O_3 NPs against (a) *Staphylococcus aureus*, (b) *Pseudomonas aeruginosa*, (c) *Klebsiella pneumonia*, and (d) *Escherichia coli*.

damage the enzymes of bacteria, which further induces cell death [21, 22]. It has been reported that green synthesized nanoparticles show enhanced antimicrobial activity compared to chemically synthesized or commercial nanoparticles because, in general, most of the plants used for synthesis nanoparticles have antimicrobial properties [23].

4. Conclusion

Green synthesis of iron nanoparticles using plant extracts is a promising method for obtaining environmentally friendly nanomaterials for biological applications. Iron oxide nanoparticles (α- Fe_2O_3) were synthesized using hibiscus flower extract as a reducing and stabilizing agent. The microwave method was successfully used for the synthesis of iron oxide nanoparticles. The microwave method has advantages. These include rapid heating, environmentally friendly and low cost, higher yield and shorter reaction time, and size and shape distribution control. Particle morphology and size were studied using TEM and XRD techniques. FTIR measurements confirmed the attachment of compounds present in the extract to the iron nanoparticles. The functional groups found in phenolic compounds can help in the formation of metallic nanoparticles. Green synthesis of metals and their oxide materials nanoparticles using plant extract is an area that needs to be explored more.

The synthesized nanoparticles were tested for their effect as antimicrobial agents against various bacteria such as *Escherichia coli*, *Staphylococcus aureus*, *Pseudomonas*, and *Klebsiella pneumonia*. The antibacterial activity trend suggested the relation between nanoparticle size and the number of nanoparticles present in the solution. The synthesized α- Fe_2O_3 NPs were used for antibacterial activity due to their high stability, less toxicity, and biocompatibility. We conclude that these Fe_2O_3 NPs may be used as antibacterial agents, replacing antibiotics in bacterial disease treatment and environmental applications. Further investigation is in progress to explore and compare iron nanoparticles' effects with drugs commonly used for these pathogens.

Data Availability

The data supporting this study are available from the corresponding author on reasonable request.

Conflicts of Interest

The authors declare that there are no conflicts of interest.

Acknowledgments

The authors are grateful to Prof. AKill Dakhel, Physics Department, the University of Bahrain, for his assistance on XRD. This work was supported by the School of Postgraduate Studies and Research, the Royal College of Surgeons in Ireland, and the Medical University of Bahrain.

References

[1] M. Rafique, I. Sadaf, M. S. Rafique, and M. B. Tahir, "A review on green synthesis of silver nanoparticles and their applications, artificial cells," *Nanomedicine and Biotechnology*, vol. 45, 2016.

[2] S. Saif, A. Tahir, and Y. Chen, "Green synthesis of Iron nanoparticles and their environmental applications and implications," *Nanomaterials*, vol. 6, p. 209, 2016.

[3] P. Christian, V. der Kammer, F. Baalousha, and T. Hofmann, "Nanoparticles structure, properties, preparation, and behaviour in environmental media," *Ecotoxicology*, vol. 17, pp. 326–343, 2008.

[4] J. Virkutyte and R. S. Vara, "Chapter 2 environmentally friendly preparation of metal nanoparticles," in *Sustainable Preparation of Metal Nanoparticles: Methods and Applications*, pp. 7–33, The Royal Society of Chemistry, London, UK, 2013.

[5] D. Bhattacharya and R. K. Gupta, "Nanotechnology and potential of microorganisms," *Critical Reviews in Biotechnology*, vol. 25, no. 4, pp. 199–204, 2005.

[6] M. R. Bindhu and M. Umadevi, "Synthesis of monodispersed silver nanoparticles using *Hibiscus cannabinus* leaf extract and its antimicrobial activity," *SpectroChimica Acta Part A: Molecular and Biomolecular Spectroscopy*, vol. 101, pp. 184–190, 2013.

[7] M. Sathish kumar, K. Sneha, S. W. Won, C. W. Cho, S. Kim, and Y. S. Yun, "Cinnamon zeylanica bark extract and powder mediated green synthesis of nano-crystalline silver particles and its bactericidal activity," *Colloids and Surfaces B: Biointerfaces*, vol. 73, pp. 332–338, 2009.

[8] V. K. T. Ngo, D. G. Nguyen, T. P. Huynh, and Q. V. Lam, "A low cost technique for synthesis of gold nanoparticles using microwave heating andits application in signal amplification for detecting *Escherichia coli* O157 : H7 bacteria," *Advances in*

Natural Sciences: Nanoscience and Nanotechnology, vol. 7, Article ID 035016, 2016.

[9] T. Shahwana, S. Abu Sirriaha, M. Nairata et al., "Green synthesis of iron nanoparticles and their application as a fenton-like catalyst for the degradation of aqueous cationic and anionic dyes," *Chemical Engineering Journal*, vol. 172, pp. 258–266, 2011.

[10] P. Salgado, K. Márquez, O. Rubilar, D. Contreras, and G. Vidal, "The effect of phenolic compounds on the green synthesis of iron nanoparticles (FexOy-NPs) with photocatalytic activity," *Applied Nanoscience*, vol. 9, pp. 371–385, 2019.

[11] B. Kumar, K. Smita, S. Galeas et al., "Characterization and application of biosynthesized iron oxide nanoparticles using citrus paradisi peel: a sustainable approach," *Inorganic Chemistry Communications*, vol. 119, Article ID 108116, 2020.

[12] P. N. V. K. Pallelaa, S. Ummey, L. K. Ruddaraju et al., "Antibacterial efficacy of green synthesized α-Fe_2O_3 nanoparticles using *Sida cordifolia* plant extract," *Heliyon*, vol. 5, Article ID e02765, 2109.

[13] A. Šutka, M. Vanags, A. Spule et al., "Identifying iron-bearings nanoparticles precursor for thermal transformation into the highly active hematite photo-fenton catalyst," *Catalyst*, vol. 10, p. 778, 2020.

[14] B. Kumar, "Green synthesis of gold, silver, and iron nanoparticles for the degradation of organic pollutants in wastewater," *Journal of Composites Science*, vol. 5, p. 219, 2021.

[15] Md. S. H. Bhuiyan, M. Y. Miah, S. C. Paul et al., "Green synthesis of iron oxide nanoparticle using *Carica papaya* leaf extract: application for photocatalytic degradation of remazol yellow RR dye and antibacterial activity," *Heliyon*, vol. 6, Article ID e04603, 2020.

[16] A. Yardily and N. Sunitha, "Green synthesis of iron nanoparticles using hibiscus leaf extract, characterization, antimicrobial activity," *International Journal of Scientific Research and Revie*, vol. 8, no. 7, 2019.

[17] W. Haiss, T. K. Nguyen, T. J. Aveyard, and D. G. Fernig, "Determination of size and concentration of gold nanoparticles from U.V./vis spectra," *Analytical Chemistry*, vol. 79, no. 11, pp. 4215–4221, 2007.

[18] D. A. Demirezen, S. Yilmaz, and D. D. Yilmaz, "Green synthesis and characterization of iron nanoparticles using aesculus hippocastanum seed extract," *International Journal of Advances in Science Engineering and Technology*, vol. 62 pages, 2018.

[19] A. Azam, A. S. Ahmed, M. Oves, M. S. Khan, S. S. Habib, and A. Memic, "Antimicrobial activity of metal oxide nanoparticles against gram-positive and gram-negative bacteria: a comparative study," *International Journal of Nanomedicine*, vol. 7, pp. 6003–6009, 2012.

[20] S. A. Ansari, A. Azam, and A. H. Naqvi, "Structural and morphological study of Fe_2O_3 nanoparticles," *Asian Journal of Research in Chemistry*, vol. 4, no. 10, pp. 1638–1642, 2011.

[21] B. Akbari, M. Pirhadi Tavandashti, and M. Zandrahimi, "Particle size characterization of nanoparticles–a practical approach," *Iranian Journal of Materials Science & Engineering*, vol. 8, no. 2, pp. 48–56, 2011.

[22] S. Bardhan, K. Pal, S. Roy et al., "Nanoparticle size-dependent antibacterial activities in natural minerals," *Journal of Nanoscience and Nanotechnology*, vol. 11, pp. 7112–7122, 2019.

[23] S. Kavita, J. Santhanalakshmi, and B. Viswanathan, "Green synthesis of silver nanoparticles using *Polyalthia longifolia* leaf extract along with D-sorbitol: study of antibacterial activity," *Journal of Nanotechnology*, vol. 2011, Article ID 152970, 5 pages, 2011.